Antioxidant Deactivation on Graphenic Nanocarbon Surfaces

Xinyuan Liu, Sujat Sen, Jingyu Liu, Indrek Kulaots, David Geohegan, Agnes Kane, Alex A. Puretzky, Christopher M. Rouleau, Karren L. More, G. Tayhas R. Palmore,* and Robert H. Hurt*

This article reports a direct chemical pathway for antioxidant deactivation on the surfaces of carbon nanomaterials. In the absence of cells, carbon nanotubes are shown to deplete the key physiological antioxidant glutathione (GSH) in a reaction involving dissolved dioxygen that yields the oxidized dimer, GSSG, as the primary product. In both chemical and electrochemical experiments, oxygen is only consumed at a significant steady-state rate in the presence of both nanotubes and GSH. GSH deactivation occurs for single- and multi-walled nanotubes, graphene oxide, nanohorns, and carbon black at varying rates that are characteristic of the material. The GSH depletion rates can be partially unified by surface area normalization, are accelerated by nitrogen doping, and suppressed by defect annealing or addition of proteins or surfactants. It is proposed that dioxygen reacts with active sites on graphenic carbon surfaces to produce surface-bound oxygen intermediates that react heterogeneously with glutathione to restore the carbon surface and complete a catalytic cycle. The direct catalytic reaction between nanomaterial surfaces and antioxidants may contribute to oxidative stress pathways in nanotoxicity, and the dependence on surface area and structural defects suggest strategies for safe material design.

Dr. X. Liu, S. Sen, J. Liu
Department of Chemistry
Brown University
Providence, RI, 02912, USA

Dr. I. Kulaots, Prof. R. H. Hurt, Prof. G. T. R. Palmore
School of Engineering
Institute for Molecular and Nanoscale Innovation
Brown University
Providence, RI, 02912, USA
Fax: (+1) 401-863-9120
E-mail: Tayhas_Palmore@brown.edu; Robert_Hurt@brown.edu

Dr. D. Geohegan, Dr. A. A. Puretzky, Dr. C. M. Rouleau
Center for Nanophase Materials Sciences
Oak Ridge National Laboratory
Oak Ridge, TN, USA

Prof. A. Kane
Department of Pathology and Laboratory Medicine
Institute for Molecular and Nanoscale Innovation
Brown University
Providence, RI, 02912, USA

Dr. K. L. More
Shared Research Equipment Facility
Oak Ridge National Laboratory
Oak Ridge, TN, USA

1. Introduction

There continues to be concern about potential health risks associated with some engineered nanomaterials, and a major international effort is underway to assess those risks and develop strategies for safe commercialization. Of particular concern are carbon nanotubes, based in part on recent reports of adverse biological responses in multiple in vivo studies,[1] though significant uncertainty remains in interpretation and hazard assessment.[2] Nanotubes are members of the family of graphenic carbon materials, whose structure is based primarily on sp^2-hybridized C–C bonding, and includes carbon black, graphite, glassy carbon, graphene, and its chemically modified form, graphene oxide. Although many graphene applications involve extended monolayers on substrates with little chance for human exposure, it is included in this list because other applications involve micro- and nanosheet forms that are processed as dry powders and are potentially respirable at some points in their manufacture and use. There has been extensive study of the biological interactions with some graphenic carbon materials, such as carbon black (CB) and carbon nanotubes,[1a–d,3] while the literature is quite limited for others, such as graphene and graphene oxide.[4] Comparative studies of biological reactivity across this family of related materials can help in the understanding of basic mechanisms that underlie biological responses.

An important nanotoxicity mechanism is oxidative stress,[5] defined as an imbalance between reactive oxygen species (ROS) and the physiological antioxidants that protect oxidation-sensitive biological molecules. Oxidative stress has been reported in a variety of target cells following exposure to CB,[6] graphene,[4a] and carbon nanotubes,[1d,3a,7]

though in some cases the effect has been attributed to redox-active metal impurities.[8] A useful biomarker for oxidative stress is depletion of GSH or the ratio of active reduced glutathione (GSH) to its inactive oxidized form, the dimer GSSG.[9]

Glutathione, a tripeptide of glutamate, glycine, and cysteine residues (**Figure 1**a), is the major endogenous antioxidant produced by cells. It deactivates free radical species and peroxides through donation of H$^+$ and e$^-$ by the internal cysteine thiol group in reactions that can be accelerated by glutathione peroxidases. GSH is the most abundant intracellular thiol with concentrations in the range of 2–10 mM; GSH is also the major extracellular antioxidant in lung lining fluid at approximately 0.4–0.5 mM in humans[10] where it protects lung epithelial cells against oxidant and chemical-induced toxicity.[11]

Intracellular GSH depletion following nanoparticle exposure is commonly interpreted as a marker for excess ROS production, but logically could also result from some direct GSH interaction at nanoparticle surfaces leading to loss of GSH by adsorption, binding, or heterogeneous oxidation. Here we conduct a systematic chemical and electrochemical study of direct GSH-nanomaterial interactions in simple acellular environments chosen to reveal basic pathways. Fenoglio et al.[12] studied acellular interactions between GSH and cobalt/tungsten carbide, which is a material system relevant to occupational risks among hard metal industry workers, but otherwise we are unaware of data on GSH interactions with material surfaces. Here we focus on carbon nanotubes and related graphene-family nanomaterials, which have been reported to induce oxidative stress[1d,4a,6,7b,c] and are among the most important and diverse classes of nanomaterials.
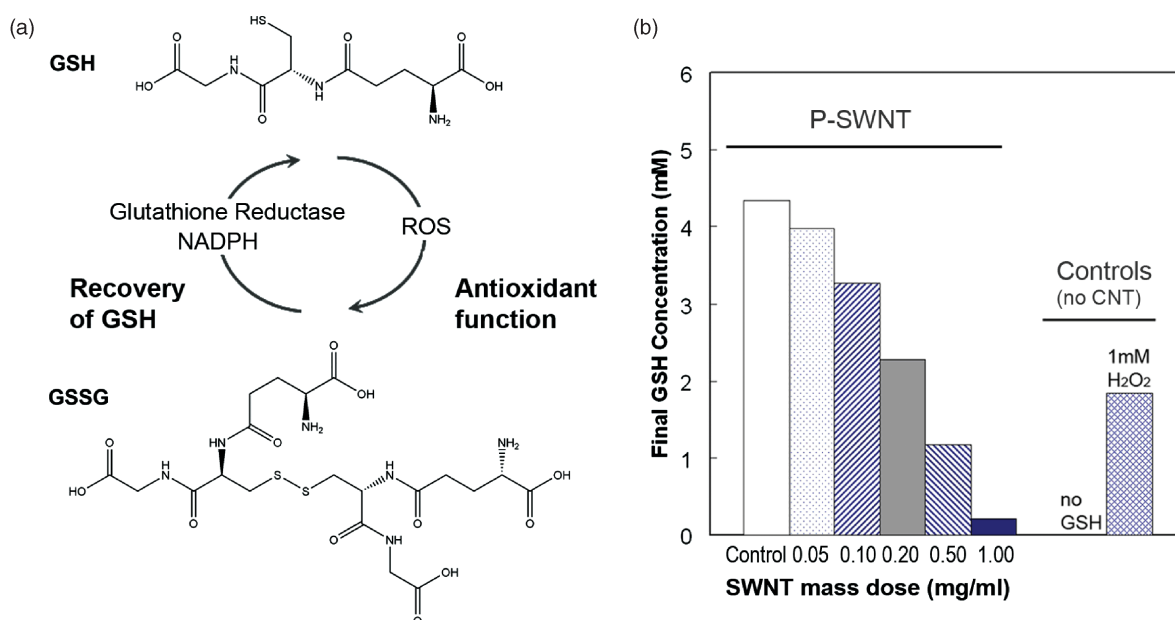
Figure 1. Glutathione structure, function, and depletion in the presence of single-walled nanotubes (SWNTs). a) Structure and physiological function of glutathione, GSH. NADPH represent nicotinamide adenine dinucleotide phosphate. b) Dose-dependent effect of purified, "P", SWNT (329 m^2/g total surface) on GSH concentration after 2-h exposure in phosphate buffered saline (PBS). 1 mM H$_2$O$_2$ serves as a positive control (CNT represent carbon nanotubes), and is shown to deplete 2 mM GSH consistent with complete reduction of H$_2$O$_2$ to water.

2. Results and Discussion

2.1. Catalytic Deactivation of Antioxidant by SWNTs

Figure 1–7 show the effects of graphenic nanocarbon surfaces on GSH concentrations in simple acellular environments measured using a thiol-sensitive fluorescent probe (see Experimental Section) applied after removal of the test nanomaterials by centrifugal ultrafiltration.[13] Figure 1b shows GSH concentration in PBS buffer after 2-h incubation with SWNTs. Nanotubes deplete GSH in a dose-dependent manner. Because SWNTs have large hydrophobic surface area, they are capable of removing small organic solutes from physiological fluids by physical adsorption.[14] To test for such reversible physical adsorption of GSH, the final CNT glutathione suspension from Figure 1b was diluted successively and allowed to come to a new equilibrium state, but GSH did not reappear in the solution. Further, time-resolved measurements (**Figure 2**a) show interaction time constants from 1 to 3000 min, inconsistent with small-molecule physical adsorption, which is typically a non-activated, fast process. The SWNT–GSH interaction appears to be a chemical reaction, and follows a first-order rate law:

$$-(d[\text{GSH}]/dt) = k[\text{GSH}][\text{CNT}] \tag{1}$$

with a rate constant, k, of 0.0084 mL mg^{-1} min^{-1} or 1.7×10^{-3} M^{-1} s^{-1} (Figure 2a dashed lines). Given sufficient time, the reaction runs essentially to completion and can be regarded as irreversible unless reductants are present (vide infra).

Figure 2b,c provide evidence that GSSG is the main reaction product. Following the SWNT-GSH depletion experiments, glutathione reductase (GR) and its cofactor, the reducing agent NADPH, are added to the system, and most of the GSH is restored. GR and NADPH are the endogenous reaction system for the restoration of GSH from its inactive oxidized form GSSG. This reduction reaction was carried out following dose-dependent GSH depletion at a constant time of 120 min (Figure 2b) and following time-dependent GSH depletion at constant SWNT dose (0.50 mg/mL) (Figure 2c). The small quantities of GSH that cannot be restored may represent higher oxidation products such as sulfenic, sulfinic, and sulfonic acids, which are unlikely to be re-reduced.[15]

Identification of GSSG as product implies oxidation. Carbon nanotubes do not typically act as oxidants, so **Figure 3** considers the possible role of dissolved O$_2$. The GSH reaction is significantly inhibited by partial deoxygenation of the buffer using N$_2$ purge (Figure 3a). Direct measurements of dissolved O$_2$ show rapid consumption when both SWNT and GSH are present (Figure 3b). Interestingly, neither SWNT nor GSH alone cause rapid oxygen consumption (Figure 3b), so all three components of this system (SWNT, GSH, O$_2$) are required to produce the reaction behavior seen in Figure 1 and 2.

It is unlikely that this surface reaction occurs by direct four-electron transfer, but rather through intermediate oxygen species either on CNT surfaces or in solution. **Figure 4** shows the effect of a variety of antioxidant enzymes and polymeric amphiphiles that could interact with reactive oxygen

(a)

(b)

(c)
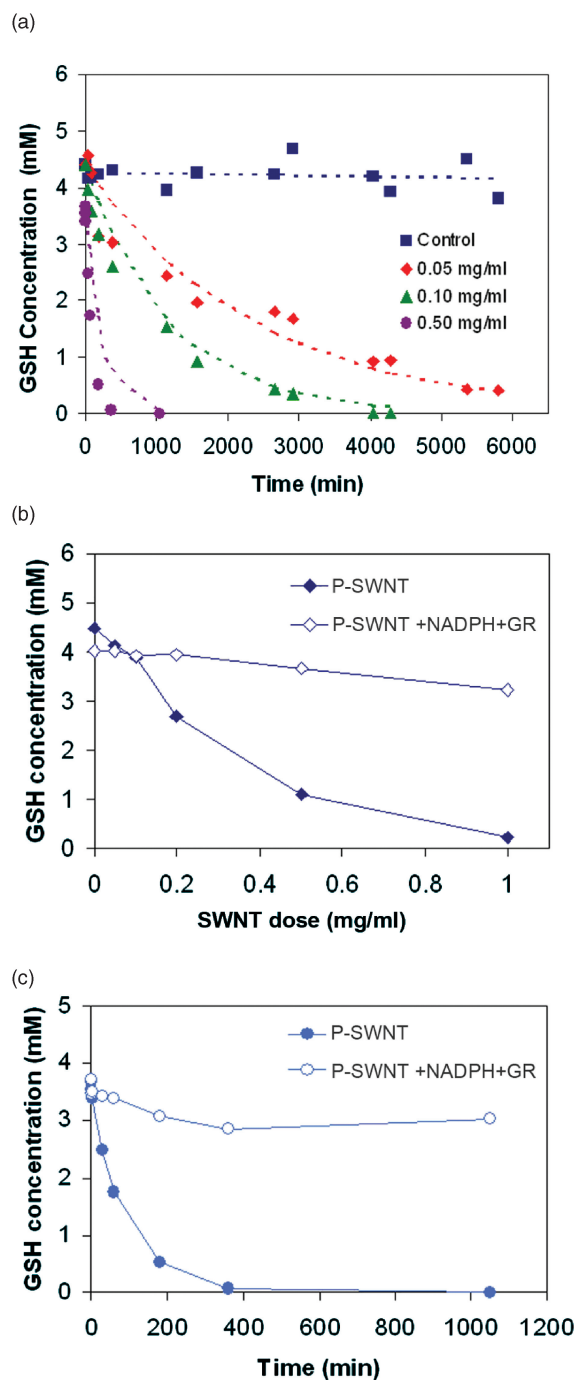
Figure 2. Behavior of the SWNT–GSH reaction. a) Time-dependence of GSH depletion induced by purified SWNTs (329 m^2/g). Long time constants indicate chemical reaction rather than physical adsorption. The first-order rate expression, $-d[\text{GSH}]/dt = k$ [GSH] [CNT] (dashed lines), gives a rate constant of $k = 0.0084$ mL mg^{-1} min^{-1} or 1.68×10^{-3} M^{-1} s^{-1}; b,c) Reversibility: GSH can be regenerated by postreaction addition of reducing agent β-NADPH (4.5 mM) and enzyme glutathione reductase (GR, 0.5 unit/mL).

intermediates. The GSH depletion reaction was partially inhibited (Figure 4a) by addition of either superoxide dismutase (SOD), an enzyme that catalyzes disproportionation of superoxide anion (O$_2^{\cdot-}$) to O$_2$ and H$_2$O$_2$, or catalase,

(a)

(b)
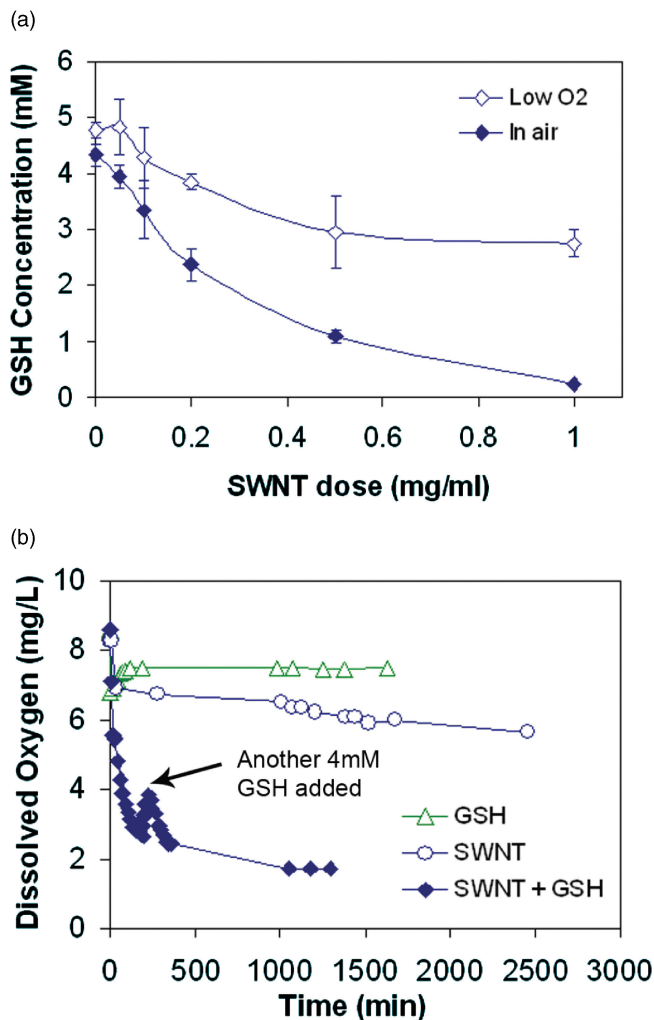
Figure 3. Role of dissolved oxygen on the SWNT–GSH reaction. a) GSH depletion is significantly inhibited under low-O_2 conditions compared with reaction in oxygen-saturated water ($p < 0.005$ for CNT dose of 1.0 mg/mL); b) dissolved oxygen is consumed quickly only when both SWCNT and GSH present are the system. Data for P-SWNT (329 m^2/g).

an enzyme selective for destruction of peroxides. Catalase is more effective, but both inhibit partially, and their effects are additive. The SOD and catalase reactions suggest the presence of superoxide and peroxide species, though nonspecific inhibition by protein adsorption on CNT surfaces is also possible.[16] Asymmetry in the electrochemical voltammograms (vida infra) also suggests that some portion of the GSH oxidation occurs away from the electrode surface, in solution, which suggests the presence of free ROS byproducts as oxidants in this homogeneous process. Figure 4b shows that the reaction is unaffected by glutathione peroxidase (GPX), whose physiological function is the reduction of H_2O_2 and certain other peroxides and hydroperoxides to water using GSH as a reductant. Based on this result, the reaction of GSH with free H_2O_2 likely occurs, but is not the overall rate-limiting step. Evidence suggests that the rate-limiting step is the formation and/or decomposition of the surface oxide (vida infra).

The present data set suggests that the rate-limiting step in the overall reaction is the formation or decomposition

(a)

(b)

(c)
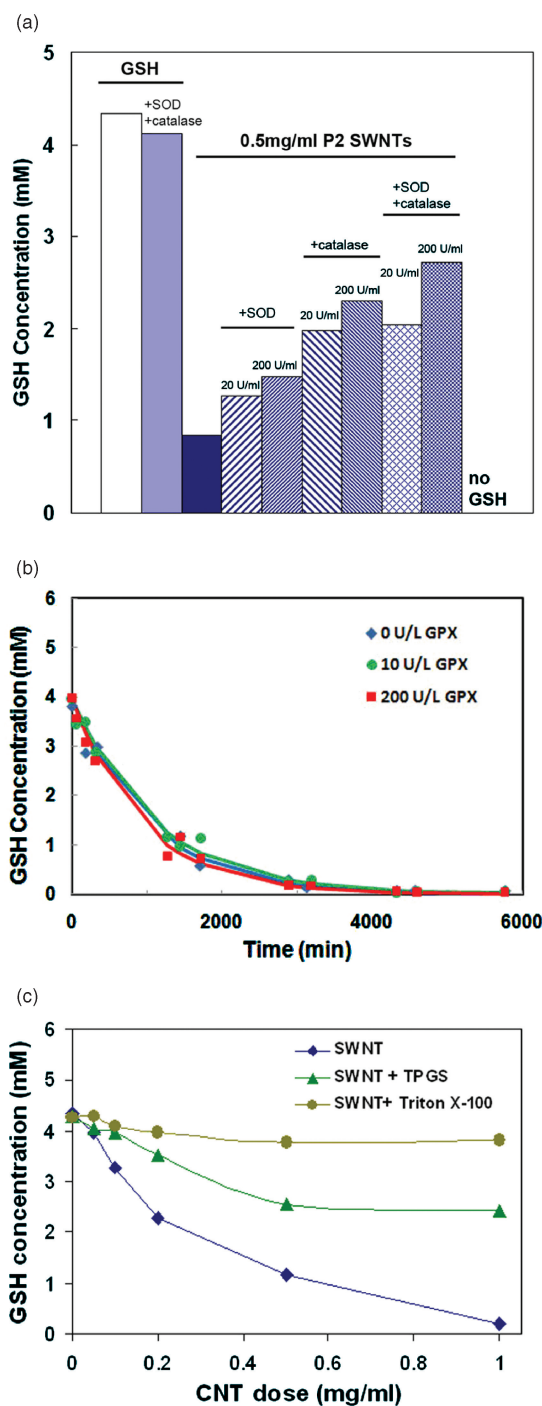
Figure 4. Effect of antioxidant enzymes and polymer coatings on the SWNT–GSH reaction. a) Antioxidant enzymes catalase and superoxide dismutase (SOD) cause partial inhibition of the SWNT-mediated GSH–O_2 reaction. b) Glutathione peroxidase (GPX) has no measurable effect. c) Two polyethylene glycol (PEG)-based amphiphilic coatings inhibit the GSH–O_2 reaction. Tocopheryl polyethylene glycol succinate (TPGS) is tocopherol conjugated to PEG, and is used as a water-soluble vitamin E formulation.[17] All data are for purified SWNTs (329 m^2/g).

of a CNT-surface-bound oxygen species. The reaction of dissolved O_2 with carbon surfaces has been widely studied, as it is relevant to fuel cell cathodes and to the behavior of activated carbon in liquid phase adsorption applications.

The aqueous reaction between O_2 and graphenic carbon surfaces is reported to form surface-bound oxygen intermediates,[18] primarily adsorbed superoxide anion, $C_s(O_2^{\cdot-})$, or hydroperoxide $C_s(OOH)$.[18a,b] Adsorbed superoxide is also reported to be the intermediate in the oxygen reduction on Pt electrodes.[19] In the absence of an applied voltage or a second reactant (such as GSH) the bound oxide tends to saturate the surface and stop further adsorption or steady-state reaction. In our data set we observe that SWNTs do not react with dissolved dioxygen at a significant steady-state rate, suggesting a stable surface intermediate. We find that SWNT zeta potentials do not rise during reaction, nor when SWNTs are incubated with dissolved oxygen alone, suggesting that the initial electron donation to oxygen does not produce free $O_2^{\cdot-}$, which would require positive charge accumulation on the nanotube surfaces. Additional evidence for surface species is relative reactivity of GSH and the smaller thiol, N-acetylcysteine (NAC). NAC is less reactive with H_2O_2 and superoxide in solution, consistent with its lower acidity (pK_a 9.5) and lower concentration of the active anion RS^-. Here, however, NAC showed a higher reactivity with carbon nanotubes (see Supporting Information) than GSH (pK 8.8), suggesting less stearic hindrance in the attack on the surface-bound peroxyl radical or superoxide anion.

Overall, the data in Figure 1–4 indicate that SWNTs act as catalysts that mediate the O_2 oxidation of GSH. Similar behavior for other biological target molecules has been reported recently by Ren et al.,[16,20] who report on that SWNTs mediating oxidative reactions with vitamin C, Trolox, cysteine, bovine serum albumin (BSA), and the ROS indicator dye H_2DCF, but did not study GSH. Zheng and Diner report on the general solution redox activity of SWNTs,[21] and Chen and Jafvert report photogenerated ROS from carboxylated SWNTs in sunlight.[22]

2.2. Relative Catalytic Activity of Various Graphenic Nanocarbons

A major goal of this study was to characterize the relative biological reactivity of different materials in the graphenic carbon family. **Figure 5** shows GSH activities for 11 materials as a function of mass dose (5a) and surface area dose (5b). At equal mass dose, activity decreases in the rank order: carbon black ~ graphene oxide ~ SWNTs ~ activated carbon > MWNTs of 35 nm diameter > carbon nanohorns > MWNTs of 140 nm ~ glassy carbon. Plotting activity by surface area dose removes much but not all of this variability (Figure 5b). At equal area dose the reaction rates fall within a factor of two with the exception of the nanohorns, which are a high-area, low-activity material. The underlying reason for low catalytic activity of nanohorns is unknown, but in contrast to other engineered, carbon-based nanoparticles, SWNHs exhibit an anomalously low pulmonary toxicity in mice.[23] This may be a result of their noncatalytic synthesis conditions, which results in high purity, and the high formation temperature that minimizes reactive edge sites. The universal band in Figure 5b shows that the mediation of GSH
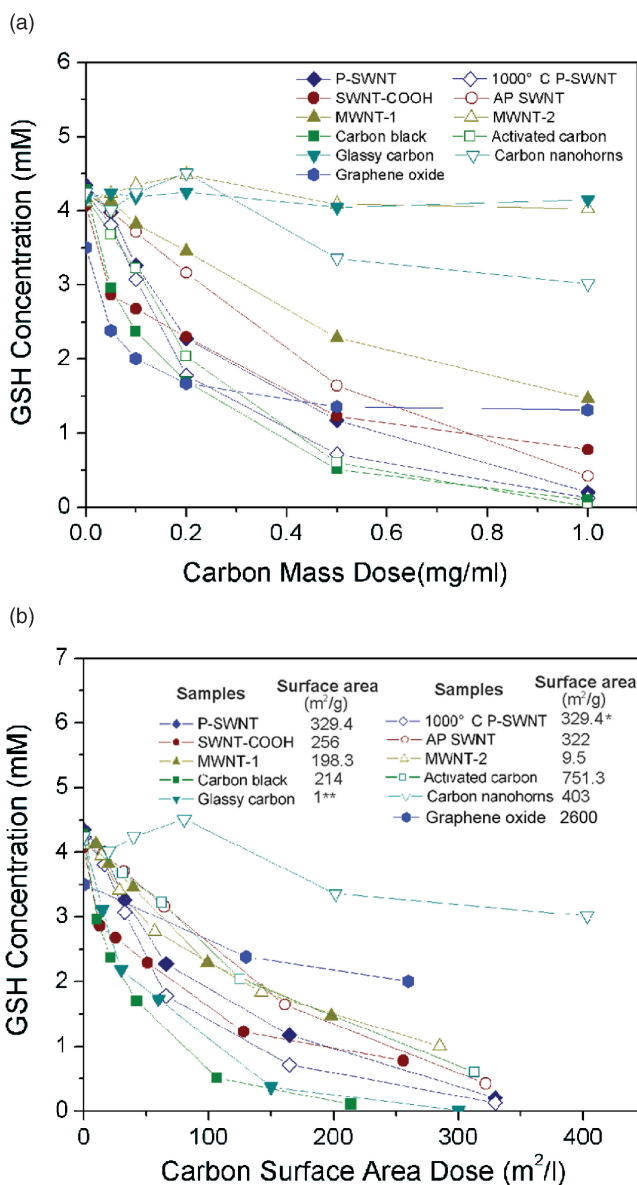
Figure 5. GSH depletion for a range of graphenic carbon materials. a) GSH depletion after 2 h incubation as a function of mass dose. MWNT represent multiwalled carbon nanotubes. b) Recasting above data as a function of surface area dose, which partially collapses the data to a near-universal curve. Surface areas in (b) by nitrogen vapor adsorption and Brunauer–Emmett–Teller (BET) theory except for glassy carbon, which is a nonporous material for which surface area can be estimated from particle size and density.

oxidation is a general property of most graphenic carbon surfaces, and emphasizes the important role of nanoparticle surface area. The primary importance of surface area has been seen for other particulate systems and has been widely reported and discussed in the general nanotoxicology literature (see e.g., Duffin et al., Oberdorster et al., Nel et al.).[5,36] The present work devoted much effort to generalizing the CNT results to other graphenic carbons. Generalization to other physiological antioxidants such as ascorbate or tocopherol requires further study.

2.3. Effect of Surface Oxidation, Annealing, and Nitrogen(N)-Doping

Carbon black was used as a model material to study annealing effects. Samples were subjected to rapid thermal annealing at 2600 °C, a temperature sufficient to transform the material to the hollow polygonal particles with planar graphene layer segments (**Figure 6**a,b) characteristic of graphitized carbon black.[24] Annealing reduces GSH activity on an equal mass basis (Figure 6c). Part of this activity loss is surface area loss, and even on an equal area basis the graphitized carbon black has a lower activity (Figure 6d) indicating that the surface-specific GSH activity is reduced due to loss of reaction sites associated with graphenic edge sites or structural imperfections or defects. Defect-mediated reactivity has also been reported for the oxygen reduction reaction on carbon electrode surfaces[18a,b] and for ROS production on MWNT surfaces.[25] In comparison, the pristine CNT sidewall has been reported to have very low rates of heterogeneous electron transfer.[26] Low concentration of active edge sites is also a possible explanation for the low reactivity of nanohorns.

Figure 6e and f compare the GSH activity of N-doped and undoped MWNTs. The N-containing tubes are more reactive at both equal mass and equal area doses. This behavior is consistent with the reported high activity of N-doped tubes in the oxygen reduction reaction.[27] Studies suggest that oxygen reduction by carbon begins with chemical adsorption of O_2 on carbon active surface sites and formation of superoxide anion $(O_2^{\cdot-})$, whose formation rate determines the catalytic activity of carbon in oxidation reactions.[18c] Results from theoretical calculations indicate that adsorption of O_2 on carbon surface becomes more energetically favorable as the extent of N-doping increases,[28] while formation of $(O_2^{\cdot-})$ on the surface was reported to be more effective for N-containing carbons.[29] Nitrogen-doped carbon nanotubes are reported to have enhanced electrochemical catalytic activity for oxygen reduction reaction.[30] Our data are consistent with this literature if $C(O_2^{\cdot-})$ or $C(OOH)$ are principle surface intermediates in the $C/O_2/GSH$ reaction as we suggest.

We have also found that severe oxidation of SWNTs with H_2SO_4/HNO_3 eliminated the GSH activity (see Supporting Information Figure S4) presumably by destroying the carbon-based catalytic active sites. Finally, most nanotubes contain metal residues of varying bioavailability,[13,31] which can serve as redox catalysts if leached into surrounding media or if the metal/metal-oxide surfaces are fluid accessible, even at low metals content.[32] To test for any effect of metal contaminants, SWNTs and carbon black were washed with 3 M HCl followed by hot water wash as described in Liu et al.,[33] but saw no significant difference (see Supporting Information, Figure S5). Also trace metal ions were removed from system by chelexing and filtration of the PBS buffer. Purified SWNTs interact with GSH identically in both untreated and treated buffer solution (see Supporting Information, Figure S5). These results indicate that the GSH reaction is not due to trace metals in PBS, nor to dissolvable trace metal on the surfaces of SWNTs or carbon black. We did not study further the potential contribution of trace metals to the catalytic activity in the larger sample set.

2.4. Electrochemical Behavior of the CNT/O_2/GSH System

To understand this reaction system in more detail, electrochemical experiments were carried out using indium tin oxide (ITO) electrodes with and without SWNT coatings, and in media with and without GSH and dissolved oxygen. Cyclic voltammograms (CVs) were obtained in a three-electrode configuration described previously.[34] Shown in **Figure 7**a are CVs of ITO electrodes with and without a coating of SWNTs in the presence or absence of GSH and O_2 in the electrolyte. The CV measured with a SWNT-coated ITO electrode exhibits a faradaic current associated with the irreversible reduction of O_2 when only O_2 is present in the electrolyte (solid-red line in Figure 7a). The onset potential of this faradaic current is –0.24 V, reaching a maximum value at ~–0.4 V. When GSH is included in the electrolyte (solid-black line in Figure 7a), significant faradaic current appears at 0.1 and –0.23 V, corresponding to the oxidation of GSH and reduction of GSSG, respectively. Both anodic and cathodic peak current increases with increasing concentration of GSH (data not shown). In addition, the faradaic current associated with the irreversible reduction of O_2 is diminished, suggesting O_2 plays a role (i.e., mediation) in the redox behavior of GSH/GSSG at SWNT. Furthermore, when an uncoated ITO electrode is used (dashed-black line in Figure 7a), faradaic current associated with either the GSH/GSSG couple or the reduction of O_2 is not observed in the CV, indicating SWNT facilitates the kinetics of heterogeneous electron transfer between the ITO electrode and the GSH peptide via activation of O_2. The remaining two control experiments confirm these conclusions, that is, the CV taken with an uncoated ITO electrode does not exhibit appreciable oxygen reduction current in the presence of O_2 (dashed-red line in Figure 7a and inset) nor does a CV taken with a SWNT-coated ITO electrode in the absence of O_2 (green line in Figure 7a inset). The asymmetry of the anodic and cathodic peaks associated with the GSH/GSSG redox couple also reveals the catalytic role of SWNT–"O_2" at oxidizing GSH to GSSG (i.e., the concentration of GSSG becomes greater than GSH, leading to a larger cathodic current).

Shown in Figure 7b are CVs of GSH/O_2 measured with a SWNT-coated ITO electrode as a function of scan rate. The inset is a plot of the maximum current for anodic and cathodic peaks in each CV as a function of scan rate. The linear dependence of peak current on the square root of scan rate indicates the faradaic current at 0.1 and –0.23 V correspond to a diffusible species in solution, specifically GSH and GSSG. Note that these experiments are not designed to develop a GSH detection method, but to give additional insight into surface mechanisms (see below).
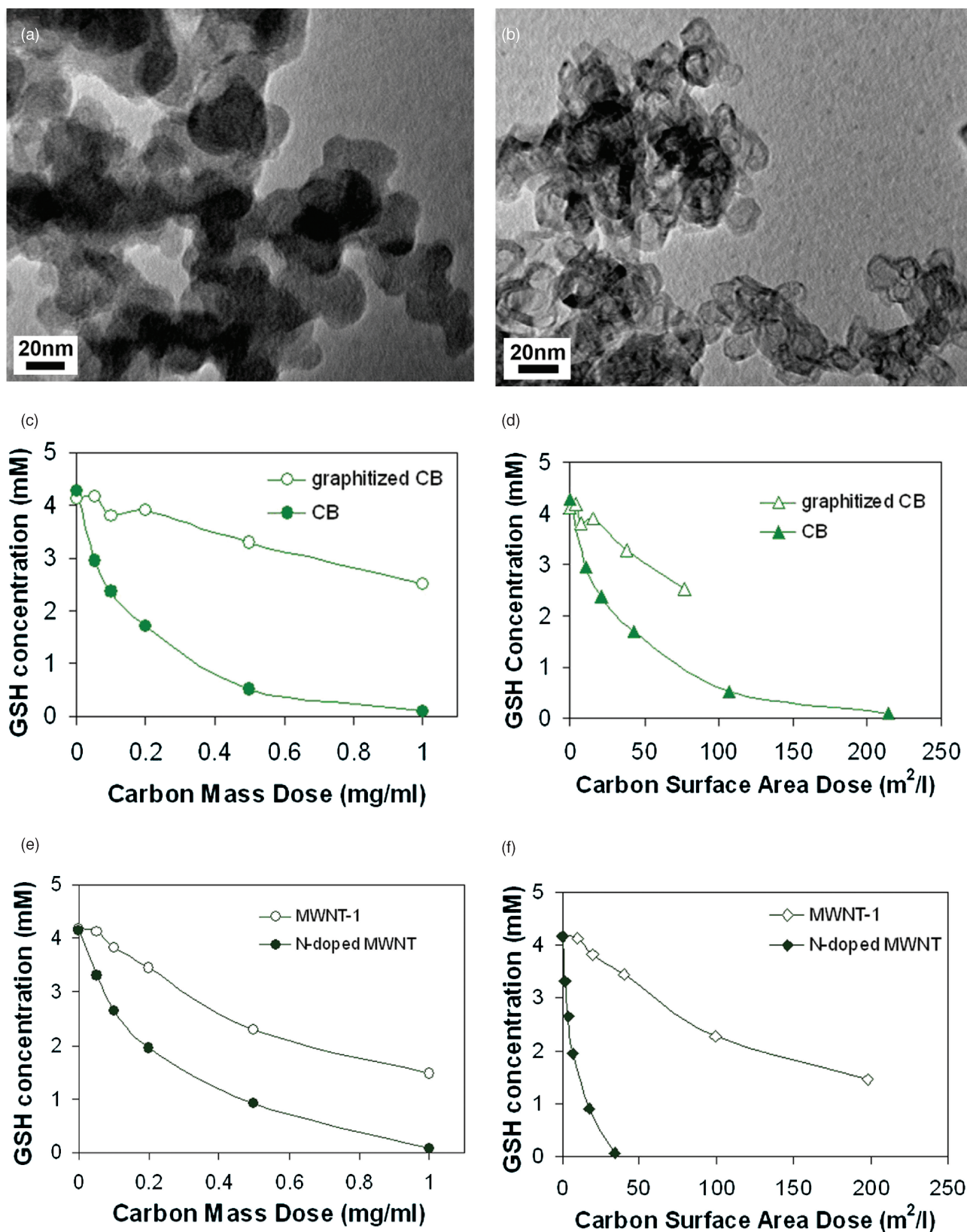
Figure 6. Effect of annealing and nitrogen doping on the GSH reactivity of carbon black surfaces and carbon nanotubes. a) TEM of as-produced carbon black; b) TEM of graphitized carbon black with characteristic hollow polygonal structure produced from (a) by annealing at 2600 °C. c) Annealing/graphitization reduces GSH reactivity on equal mass dose basis. d) Annealing/graphitization also reduces GSH reactivity on an area dose basis due to increased structural perfection and reduced defect/edge density; N-doped tubes show higher GSH oxidation reactivity both at equal mass dose (e) and area dose (f). Sample morphology shown in the Supporting Information.
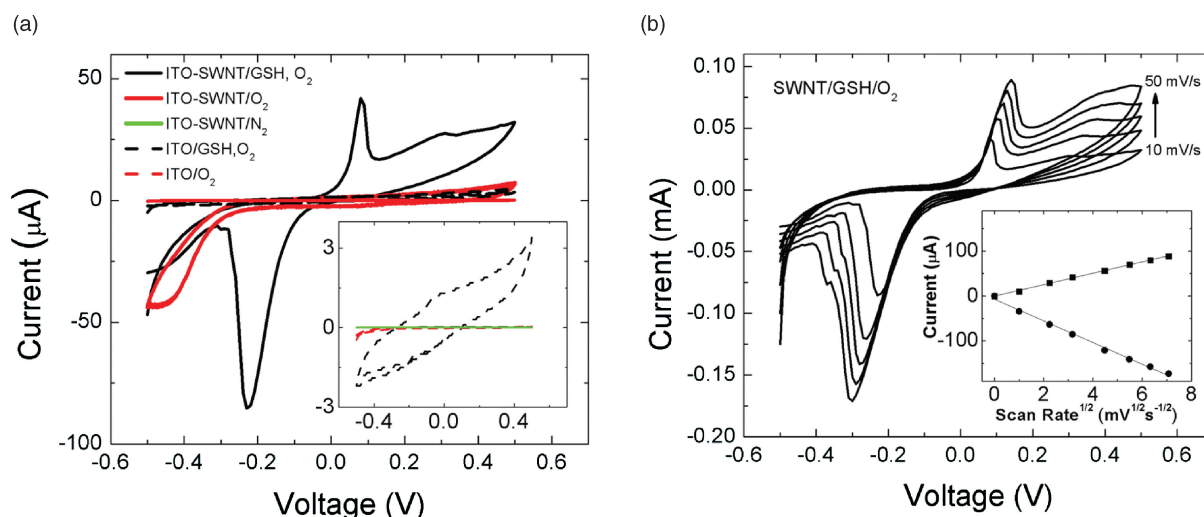
Figure 7. a) Cyclic voltammogram (CV) of glutathione/glutathione disulfide (GSH/GSSG) redox couple at an indium tin oxide (ITO) electrode coated with SWNTs. Quasi-reversible electrochemistry is indicated by the spread in the anodic and cathodic peaks centered at 0.1 and −0.23 V, respectively. CVs of control experiments are included for comparison. CV of ITO-SWNT with and without O_2 present reveals the onset potential for O_2 reduction at −0.24 V. The inset expands the CVs of the three control experiments exhibiting low currents. A lack of faradaic current in these control experiments indicates both SWNT and O_2 must be present to observe GSH/GSSG electrochemistry. The onset potentials for GSSG reduction and GSH oxidation are −0.05 and +0.05 V, respectively. Note that the region associated with O_2 reduction in this CV is depleted relative to the CV without GSH at identical concentrations of O_2. Reference electrode: Ag/AgCl; scan rate 10 mV/s, counter electrode carbon felt. b) Electrochemical behavior of the SWNT-coated $ITO/O_2/GSH$ system: effect of scan rate. Current is reduced at low scan rate indicating local reactant depletion. The linear dependence of peak current on the square root of scan rate indicates the rate-limiting electrochemical process involves diffusible GSH/GSSG. All data are for purified SWNTs (329 m^2/g).

2.5. Reaction Mechanism

Based on these results, we propose the catalytic mechanism shown in **Figure 8**. Graphenic carbon surfaces interact with dissolved dioxygen to form a surface-bound $C(O_2)$ intermediate, which oxidizes GSH to GSSG as the major product and restores the carbon surface to its original state. The literature suggests that the reaction takes place selectively on active sites, which are graphenic edge or defect sites[18a,35] in agreement with our annealing data, and there is evidence that the bound species is superoxide or hydroperoxyl[18a,b] with the rate limiting step below pH 9 being initial O_2 reduction[18a] consistent with involvement of a diffusible species in our frequency-dependent voltammograms. There is evidence that free ROS are byproducts of this heterogeneous process, typically superoxide or the two-electron reduction product, hydrogen peroxide, and these ROS carry out further oxidation of GSH in solution by known homogeneous chemical routes (Figure 8).

Acellular GSH depletion may be an attractive simple assay for the oxidative activity of carbon-based materials, as it gives consistent results that reveal material-to-material differences across the graphenic material family and does not suffer from artifacts associated with dye adsorption. Adsorption of dyes or electron paramagnetic resonance (EPR) spin probes to hydrophobic surfaces have been cited as technical limitations of conventional assays for oxidative activity of nanomaterials.[9] In conventional assays such as the 2′,7′-dichlorodihydrofluorescin (DCFH) assay, conjugated dye molecules necessarily come into direct contact with graphenic carbon surfaces,[9] and physical adsorption

with quenching can cause underestimation of surface oxidative activity. The GSH assay may also have advantages over EPR techniques, which detect free radical oxidants,[37] but may not detect all oxygen-containing surface-bound intermediates that define the main pathway for carbon-catalyzed biological oxidation processes.[20] In the absence of GSH, we observe no O_2 consumption, which is consistent with reports of negligible ROS generation from nanotubes in some acellular assays that are predicated on the generation of solution-phase ROS. Note that these experiments do not attempt to simulate the intracellular GSH depletion process, which is a dynamic response to multiple oxidative pathways in the complex cellular environment.

3. Conclusion

This study demonstrates for the first time the ability of carbon nanomaterials to deactivate antioxidants through direct surface reaction involving bound oxygen intermediates. This route can contribute to oxidative stress pathways and toxicity for carbon nanotubes, but is not unique to CNTs. Rather, it is a pathway common to a wide range of graphenic carbon materials that include carbon black, activated carbons, and graphene oxide. The reaction is dependent on total surface area and mediated by structural defects. This toxicity pathway can be suppressed as a safe design strategy by high-temperature annealing, which typically reduces both defect density and total surface area. This acellular reaction is not intended as a method to predict intracellular GSH depletion in nanotoxicity studies, but can be used as a basic chemical assay of oxidative potential for a test material, and in this
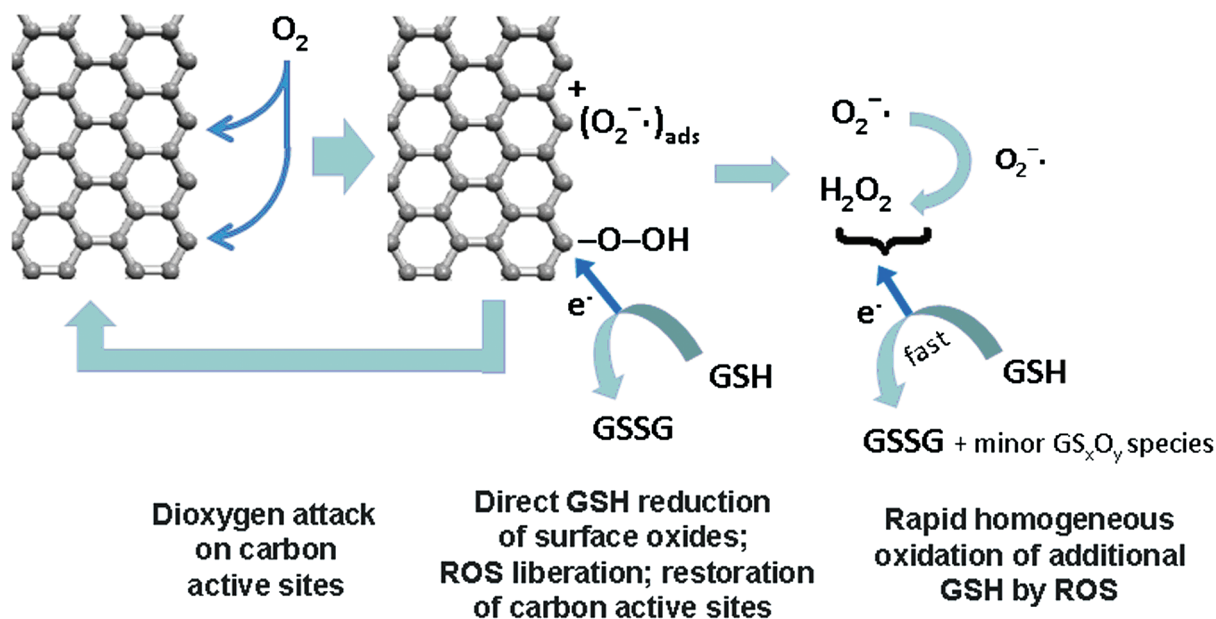
Figure 8. Proposed reaction mechanism: carbon nanomaterial surfaces as catalysts for the glutathione dioxygen reaction. Carbon surfaces react with dissolved dioxygen to form surface-bound intermediates that oxidize GSH to GSSG and minor GS_xO_y byproducts. There is evidence that part of the GSH oxidation occurs in solution by ROS intermediates of the primary heterogeneous reaction.

role it does not suffer from interferences associated with indicator dye adsorption on carbon surfaces that are possible with other chemical assays.

4. Experimental Section

Materials: A panel of carbon nanomaterials were assembled from different sources. Arc-synthesized purified SWNTs with low functionality (P-SWNT) and carboxylic functionalized (SWNT-COOH) were obtained from CSI, Riverside, CA ("P2" and "P3" products, respectively). The purification was performed by air oxidation followed by acid etching of the catalyst and annealing to restore the low-functional group inventory similar to pristine tubes. The final product has 4–7 wt% Ni-Y by thermogravimetric analysis (TGA). The functional groups left by acid washing are not removed in "P3" grade giving 1–3 at% carboxylic acid in the hydrophilic product (and 5–8 wt% metal). MWNTs (MER, Tuscon, AZ) in the form of spherical aggregates with diameter of 140 ± 30 nm and length ca 7 ± 2 μm (MWNT-1, purity of >90%) and long MWCNTs with diameter of 35 ± 10 nm and length of 30 μm (MWNT-2, 90% purity, <0.1% iron); nitrogen-doped MWNTs was a gift from Prof. Mauricio Terrones; carbon black (M4750, Cabot Corp., Billerica, MA); activated carbon (Calgon Carbon Corp., Pittsburgh, PA) and glassy carbon (SPI, West Chester, PA). Single-wall carbon nanohorns (SWNHs) were produced by high-power Nd:YAG laser vaporization of pure graphite into background Ar gas at high temperature (1100 °C)

as described previously.[38] The short-SWNHs (s-SWNHs) used in these studies were produced by minimizing the laser pulse widths (0.5 ms, 4.5 J/pulse, 80 Hz), yielding nanohorns with individual lengths <10 nm and roughly spherical aggregates with diameters typically between 40–60 nm, as assessed by high-resolution transmission electron microscopy (Hitachi, HF-3300 at 300 kV). The growth time above 1000 °C was limited to 8 ms, followed by several seconds annealing time at 1000 °C within the tube furnace. As-produced SWNTs were produced in the same laser vaporization reactor under nearly identical conditions however with a Ni/Co/C target (1:1:98 at%), yielding nanotubes with diameters ranging 1.2–1.4 nm. Bioavailable metals from as-produced SWNTs and carbon black were removed by 3 M HCl and following hot water washes as described previously.[33] Graphitized carbon nanoparticles were carried out by heating carbon black at 2600 °C under N_2 gas protection for 1 min in a custom-built resistive heat treatment device.[39] Highly oxidized amorphous carbon was prepared by agitating ca 60 mg purified SWNTs in 100 mL mixed acid solutions (98% H_2SO_4: 70% HNO_3 = 3:1) for 5 h.

Reduced glutathione (GSH), oxidized glutathione (GSSG), glutathione reductase (GR), β-nicotinamide adenine dinucleotide 2′-phosphate reduced tetrasodium salt hydrate (β-NADPH), superoxide dismutase (SOD), catalase, *N*-acetylcysteine (NAC) were purchased from Sigma Chemicals Co. (St. Louis, MO). Hydrogen peroxide (30%) was purchased from Fisher Scientific Inc. (Pittsburgh, PA). ThioGlo-1, a maleimide reagent that produces

a highly fluorescent adduct upon reaction with thiol groups, was purchased from Calbiochem, Inc. (San Diego, CA). Food-grade tocopheryl polyethylene glycol succinate (TPGS-1000, molecular weight: ~1513 Da) was obtained from Eastman Chemical Company (Llangefni, UK) and Triton X-100 was purchased from Alfa Aesar (Ward Hill, MA).

Characterization: Morphologies of carbon nanomaterials were characterized using a Philips 420 transmission electron microscopy (TEM) using an accelerating voltage of 120 kV and a JEOL 2010 high-resolution transmission electron microscope (HRTEM) at 200 kV. Total surface areas were measured by nitrogen vapor adsorption at 77 K (Autosorb-1, Quantachrome, Boynton Beach, Florida) determined from the Brunauer, Emmett, and Teller (BET) method. Depending upon the approximate surface area of the sample, 30 mg to 200 mg of carbon nanomaterial powder was placed into a sample vial and out-gassed at 300 °C overnight to clean the surface. Twelve data point nitrogen isotherm was obtained to calculate the BET surface area of the sample. The BET surface area of the char samples was determined over the partial pressure (P/P_o) range where the BET equation had the highest correlation coefficient (at least 0.9999). For most non-microporous samples, the commonly accepted range of P/P_o for BET equation is from 0.05 to 0.3.

Carbon-GSH Interactions: 4 mM reduced glutathione was added to 0.05–1.0 mg/mL of carbon nanomaterials suspended in PBS buffer, and the mixture was sonicated in water bath for 15 min and then agitated on a rotator in room light for the desired reaction time. After that the suspension was transferred to a ultrafiltration centrifuge tube (3000 NMWL Amico centrifugal filter devices, Millipore, MA) and subjected to 30 min of centrifugation to remove the nanomaterials[13] and any other solids to obtained a clear filtrate. GSH concentrations in filtrate were determined with ThioGlo-1 fluorescent reagent. ThioGlo-1 reagent aliquots of 20 mM were prepared by diluted as-received solids with dimethyl sulfoxide (DMSO). A calibration curve of GSH was established by adding 1.0–5.0 μL of 4.0 mM GSH to 5.0 mL PBS buffer (pH 7.4) containing 20 μM ThioGlo-1 (DMSO solution). Sample solutions were obtained by the addition of 5.0 μL CNT filtrates to 5.0 mL PBS with 20 μM ThioGlo-1 in dark room. After 30 min reaction with dye solution, 200 μL standards or filtrate samples were transferred into a 96-well plate and assayed for fluorescence on SpectraMax M2 using excitation at 379 nm and emission at 513 nm. To study the role of oxygen, this experiment was also carried out in glove box using deoxygenated GSH PBS solution, which was purged with N_2 overnight. The kinetic study was performed by agitating different concentrations of CNTs in suspension (0.05, 0.10, and 0.50 mg/mL) with GSH from 1 min up to 100 h. Dissolved oxygen concentration in PBS buffer was measured with a DO probe 083010MD on a ThermoOrion 5-star plus portable multiparameter Meter (Thermo Scientific, Beverly, MA) with addition of P2 SWNT, GSH, or SWNT plus GSH in a sealed glass bottle with strong magnetic stirring. Oxidized glutathione (GSSG) concentration was measured by reducing it to GSH using β-NAPDH and glutathione reductase (GR), and then assayed with ThioGlo-1. To evaluate the reducing efficacy of NAPDH and glutathione reductase (GR) for GSSR, 2 mM GSSG PBS solution and 4.5 mM β-NADPH, 0.5 unit/mL GR were mixed and allowed to react for at least 5 min, and then 0–5 μL mixed solution was added into 5 mL PBS solution containing 20 μM ThioGlo-1 (DMSO solution), and then after vortex mixing, wait 30 min reaction before assayed for fluorescence. Similarly, GSSG concentrations in sample

solutions were also determined using ThioGlo-1 by addition of β-NADPH and GR. For the reaction inhibition experiments, 20 or 200 unit/mL superoxide dismutase (SOD), catalase or both were added into CNT suspensions with 4 mM GSH, and then after 15 min sonication and 2 h mild agitation, filtrates were obtained from ultra-centrifugation and assayed for GSH concentrations. To evaluate if surfactants will inhibit this interaction, TPGS and Triton-100 were prepared according to Yan et al.,[17] and then TPGS or Triton-100 was added into CNT suspensions of concentration of 0.05–1.0 mg/mL with 4 mM GSH, and then the samples were filtrated and GSH concentrations were assayed with ThioGlo-1.

Electrochemical Experiments: A SWNT suspension of 1.0 mg/mL was dispersed in dimethylformamide (DMF) and sonicated in water bath for 30 min, then diluted to 0.5 mg/mL and sonicated 30 min, then successively diluted to 0.1 mg/mL and sonicated for 1 h. All experiments were performed with a three-electrode configuration using an Ag/AgCl reference electrode, carbon felt, or platinum gauze as the counter electrode as specified, and ITO-coated glass ($10 \times 10 \times .55$ mm) as the working electrode. The catalytic surface was prepared by depositing 60 μL of a 0.1 mg/mL dispersion of the SWNT dispersion in DMF and subsequent drying at 40 °C. The SWNT dispersion was sonicated for an hour prior to use. A 4 mM solution of glutathione in phosphate buffer solution was used for all the studies. Inert gases (N_2/Ar) used for purging were bubbled in the solution for 30 min for each attempted observation. Cyclic voltammetry was performed from −0.5 to +0.5 V at a scan rate of 10 mV/s unless specified.

Supporting Information

Supporting Information is available from the Wiley Online Library or from the author.

Acknowledgements

[1] a) C. A. Poland, R. Duffin, I. Kinloch, A. Maynard, W. A. H. Wallace, A. Seaton, V. Stone, S. Brown, W. MacNee, K. Donaldson. *Nat. Nanotechnol.* **2008**, *3*, 423–8; b) A. Takagi, A. Hirose, T. Nishimura, N. Fukumori, A. Ogata, N. Ohashi, S. Kitajima, J. Kanno, *J. Toxicol. Sci.* **2008**, *33*, 105–116; c) J. P. Ryman-Rasmussen, M. F. Cesta, A. R. Brody, J. K. Shipley-Phillips, J. I. Everitt, E. W. Tewksbury, O. R. Moss,

B. A. Wong, D. E. Dodd, M. E. Andersen, J. C. Bonner, *Nat. Nanotechnol.* **2009**, *4*, 747–751; d) A. A. Shvedova, E. Kisin, A. R. Murray, V. J. Johnson, O. Gorelik, S. Arepalli, A. F. Hubbs, R. R. Mercer, P. Keohavong, N. Sussman, J. Jin, J. Yin, S. Stone, B. T. Chen, G. Deye, A. Maynard, V. Castranova, P. A. Baron, V. E. Kagan, *Am. J. Physiology–Lung Cellular Mol. Phys.* **2008**, *295*, L552–L565; e) D. W. Porter, A. F. Hubbs, R. R. Mercer, N. Wu, M. G. Wolfarth, K. Sriram, S. Leonard, L. Batelli, D. Schwegler-Berry, S. Friend, M. Andrew, B. T. Chen, S. Sturuoka, M. Endo, V. Castranova, *Toxicology* **2010**, *269*, 136–147; f) R. R. Mercer, A. F. Hubbs, J. F. Scabilloni, L. Wang, L. A. Battelli, D. Schwegler-Berry, V. Castranova, D. W. Porter, *Part Fibre Toxicol* **2010**, *7*, 28.

[2] a) C. Varga, K. Szendi, *In Vivo* **2010**, *24*, 153–156; b) J. Muller, M. Delos, N. Panin, V. Rabolli, F. Huaux, D. Lison, *Tox. Sci.* **2009**, *110*, 442–448.

[3] a) S. K. Manna, S. Sarkar, J. Barr, K. Wise, E. V. Barrera, O. Jejelowo, A. C. Rice-Ficht, G. T. Ramesh, *Nano Lett.* **2005**, *5*, 1676–84; b) A. Elder, R. Gelein, J. N. Finkelstein, K. E. Driscoll, J. Harkema, G. Oberdörster, *Toxicol. Sci.* **2005**, *88*, 614–629.

[4] a) Y. Zhang, S.F. Ali, E. Dervishi, Y. Xu, Z. Li, D. Casciano, A. S. Biris, *ACS Nano* **2010**, *4*, 3181–3186; b) O. Akhavan, E. Ghaderi, *ACS Nano* **2010**, *4*, 5731–5736; c) X. M. Sun, Z. Liu, K. Welsher, J. T. Robinson, A. Goodwin, S. Zaric, H. J. Dai, *Nano Res.* **2008**, *1(3)*, 203–212; d) E. C. Salas, Z. Z. Sun, A. Luttge, J. M. Tour, *ACS Nano* **2010**, *4*, 4852–4856.

[5] a) A. Nel, T. Xia, L. Madler, N. Li, *Science* **2006**, *311*, 622–627; b) G. Oberdorster, E. Oberdorster, J. Oberdorster, *Environ. Health. Persp.* **2005**, *113(7)*, 823–839.

[6] S. Hussain, S. Boland, A. Baeza-Squiban, R. Hamel, L. C. Thomassen, J. A. Martens, M. A. Billon-Galland, J. Fleury-Feith, F. Moisan, J. C. Pairon, F. Marano, *Toxicology* **2009**, *260*, 142–149.

[7] a) A. Magrez, S. Kasas, V. Salicio, N. Pasquier, J. W. Seo, M. Celio, S. Catsicas, B. Schwaller, L. Forro, Cellular *Nano Lett.* **2006**, *6*, 1121–1125; b) C. S. Sharma, S. Sarkar, A. Periyakaruppan, J. Barr, K. Wise, R. Thomas, B. L. Wilson, G. T. Ramesh, *J. Nanosci. Nanotechnol.* **2007**, *7*, 2466–2472; c) A. A. Shvedova, V. Castranova, E. R. Kisin, D. Schwegler-Berry, A. R. Murray, V. Z. Gandelsman, A. Maynard, P. Baron, *J. Toxicol. Environ. Health A* **2003**, *66*, 1909–1926.

[8] a) V. E. Kagan, Y. Y. Tyurina, V. A. Tyurin, N. V. Konduru, A. I. Potapovich, A. N. Osipov, E. R. Kisin, D. Schwegler-Berry, R. Mercer, V. Castranova, A. A. Shvedova, *Toxicol. Lett.* **2006**, *165*, 88–100; b) S. Koyama, Y. A. Kim, T. Hayashi, K. Takeuchi, C. Fujii, N. Kuroiwa, H. Koyama, T. Tsukahara, M. Endo, *Carbon* **2009**, *47*, 1365–1372.

[9] V. Stone, H. Johnston, R. P. Schins, *Crit. Rev. Toxicol.* **2009**, *39*, 613–626.

[10] a) M. L Circu, T. Y. Aw, *Free Rad. Res.* **2008**, *42*, 689–706; b) A. M. Cantin, S. L. North, R. C. Hubbard, R. G. Crystal, *J. Appl. Physiol.* **1987**, *63*, 152–157.

[11] D. P. Jones, L. A. S. Brown, P. Sternburg, *Toxicology* **1995**, *105*, 267–274.

[12] I. Fenoglio, I. Corazzari, C. Francia, S. Bodoardo, B. Fubini, *Free Radic. Res.* **2008**, *42*, 737–745.

[13] X. Liu, V. Gurel, D. Morris, D. W. Murray, A. Zhitkovich, A. B. Kane, R. H. Hurt, *Adv. Mater.* **2007**, *19*, 2790–2796.

[14] a) L. Guo, A. Von Dem Bussche, M. Buechner, A. B. Kane, R. H. Hurt, *Small* **2008**, *4*, 721–727; b) J. M. Worle-Knirsch, K. Pulskamp, H. F. Krug, *Nano Lett.* **2006**, *6*, 1261–1268; c) A. Casey, M. Davoren, E. Herzog, F. M. Lyng, H. J. Byrne, G. Chambers, *Carbon* **2007**, *45*, 34–40.

[15] C. C. Winterbourn, D. Metodiewa, *Free Radic. Bio. Med.* **1999**, *27*, 322–328.

[16] L. Ren, H. K. Kim, W. Zhong, *Anal. Chem.* **2009**, *81*, 5510–5516.

[17] A. Yan, A. V. D. Bussche, A. B. Kane, R. H. Hurt, *Carbon.* **2007**, *45*, 2463–2470.

[18] a) H. H. Yang, R. L. McCreery, *J. Electrochem. Soc.* **2000**, *147*, 3420–3428; b) D. Qu, *Carbon* **2007**, *45*, 1296–1301; c) V. V. Strelko, N. T. Kartel, I. N. Dukhno, V. S. Kuts, R. B. Clarkson, B. M. Odintsov, *Surf. Sci.* **2004**, *548*, 281–290; d) L. R. Radovic, in *Carbon Materials for Electrochemical Energy Storage Systems: Advanced Materials and Technologies* (Eds: F. Béguin, E. Frackowiak), CRC Press (Taylor&Francis), Boca Raton, USA **2008**, pp 163–219.

[19] M. Shao, P. Liu, R. R. Adzic, *J. Am. Chem. Soc.* **2006**, *128*, 7408–7409.

[20] L. Ren, W. Zhong, *Environ. Sci. Technol.* **2010**, *44*, 6954–6958.

[21] M. Zheng, B. A. Diner, *J. Am. Chem. Soc.* **2004**, *126*, 15490–15494.

[22] C. Y. Chen, C. T. Jafvert, *Environ. Sci. & Technol.* **2010**, *44*, 6674–6679.

[23] R. M. Lynch, B. H. Voy, D. F. Glass, S. M. Mahurin, B. Zhao, H. Hu, A. M. Saxton, R. L. Donnell, M.-D. Cheng, *Nanotoxicology* **2007**, *1*, 157–166.

[24] J. S. Speck, *J. Appl. Phys.* **1990**, *67*, 495–500.

[25] J. Muller, F. Huaux, A. Fonseca, J. B. Nagy, N. Moreau, M. Delos, E. Raymundo-Pinero, F. Beguin, M. Kirsch-Volders, I. Fenoglio, B. Fubini, D. Lison, *Chem. Res. Toxicol.* **2008**, *21*, 1698–1705.

[26] a) C. E. Banks, T. J. Davies, G. G. Wildgoose, R. G. Compton, *Chem. Commun.* **2005**, 829–841; b) S. Sanchez, E. Fabregas, H. Iwai, M. Pumera, *Phys. Chem. Chem. Phys.* **2009**, *11*, 182–186; c) T. J. Davies, M. E. Hyde, R. G. Compton, *Angew. Chem. Int. Ed.* **2005**, *117*, 5121–5126.

[27] S. Maldonado, K. J. Stevenson, *J. Phys. Chem. B* **2005**, *109*, 4707–4716.

[28] Y. Okamoto, *Appl. Surf. Sci.* **2009**, *256*, 335–341.

[29] B. Stohr, H. P. Boehm, R. Schlogl, *Carbon* **1991**, *29*, 707–720.

[30] a) K. P. Gong, F. Du, Z. H. Xia, M. Durstock, L. M. Dai, *Science* **2009**, *323*, 760–764; b) Y. F. Tang, B. L. Allen, D. R. Kauffman, A. Star, *J. Am. Chem. Soc.* **2009**, *131*, 13200–13201.

[31] L. Guo, D. G. Morris, X. Liu, C. Vaslet, R. H. Hurt, A. B. Kane, *Chem. Mater.* **2007**, *19*, 3472–3478.

[32] M. Pumera, Y. Miyahara, *Nanoscale* **2009**, *1*, 260–265.

[33] X. Liu, L. Guo, D. Morris, A. B. Kane, R. H. Hurt, *Carbon* **2008**, *46*, 489–500.

[34] a) S. K. Kim, S. Sen, H. K. Song, G. T. R. Palmore, *Electrochem. Commun.* **2010**, *12*, 761–764; b) S. Y. Rhieu, D. R. Ludwig, V. S. Siu, G. T. R. Palmore, *Electrochem. Commun.* **2009**, *11*, 1857–1860.

[35] a) R. J. Bowling, R. T. Packard, R. L. McCreery, *J. Am. Chem. Soc.* **1989**, *111*, 1217–1223; b) R. R. Moore, C. E. Banks, R. G. Compton, *Anal. Chem.* **2004**, *76*, 2677–2682.

[36] R. Duffin, L. Tan, D. Brown, V. Stone, K. Donaldson, *Inhal. Toxicol.* **2007**, *19*, 849–856.

[37] I. Fenoglio, M. Tomatis, D. Lison, J. Muller, A. Fonseca, J. B. Nagy, B. Fubini, *Free Radic. Biol. & Med.* **2006**, *40*, 1227–1233.

[38] a) D. B. Geohegan, A. A. Puretzky, D. Styers-Barnett, H. Hu, B. Zhao, H. Cui, C. M. Rouleau, G. Eres, J. J. Jackson, R. F. Wood, S. Pannala, J. C. Wells, *Phys Status Solid B* **2007**, *244*, 3944–3949; b) A. A. Puretzky, D. J. Styers-Barnett, C. M. Rouleau, H. Hu, B. Zhao, I. N. Ivanov, D. B. Geohegan, *Appl. Phys. A: Mater. Sci. Process.* **2008**, *93*, 849–855; c) M. D. Cheng, D. W. Lee, B. Zhao, H. Hu, D. J. Styers-Barnett, A. A. Puretzky, D. W. DePaoli, D. B. Geohegan, E. A Ford, P. Angelini, *Nanotechnology* **2007**, *18*, 185604.

[39] H. S. Shim, R. H. Hurt, *Energy & Fuels* **2000**, *14*, 340–348.